Journal of
Intelligent Material
Systems and Structures

Original Article

Journal of Intelligent Material Systems and Structures
2017, Vol. 28(9) 1160–1174

DOI: 10.1177/1045389X16667549
journals.sagepub.com/home/jim
SAGE

A new approach for structural damage detection exploring the singular spectrum analysis

Mario A de Oliveira[1], Jozue Vieira Filho[2], Vicente Lopes Jr[3] and Daniel J Inman[4]

Abstract

This article presents a novel approach for damage detection applied to structural health monitoring systems exploring the residues obtained from singular spectrum analysis. In this technique, a lead zirconate titanate patch acting as actuator excites the structure, and three other patches are used as sensors to receive the structural responses. This method is based on a high-frequency excitation range in order to overcome the problem caused when the low-vibration modes are excited. In this method, a wideband chirp signal, with low amplitude and variable frequency, is used to excite the structure. The response signals are acquired in the time domain, and the singular spectrum analysis procedure is performed. The residues obtained between the reconstructed and original time series are used to compute statistical metrics. The residues calculated from singular spectrum analysis are used to compute the root mean square deviation and correlation coefficient deviation metric indices, rendering the damage detection approach more reliable. Tests were carried out on an aluminum plate, and the results have demonstrated the effectiveness of the proposed method making it an excellent approach for structural health monitoring applications. The results exploring different numbers of components used during the reconstruction process of time series are obtained, and the highlights are presented.

Keywords

Structural health monitoring, time series analysis, residues, statistical signal processing, principal component analysis, lead zirconate titanate

Introduction

Nondestructive evaluation (NDE) methods applied to structural health monitoring (SHM) have been growing in the last decades due to the ability of these methods to identify different kinds of damage in several types of structures working under various loading and environmental conditions. Continuous evaluation of structures aiming to prevent faults must be conducted based on different operational conditions.

Techniques based on lead zirconate titanate (PZT) have been developed in a large number of SHM applications. Here, we comment on two popular methods as a detailed discussion of all methods requires a review paper. The two methods are electromechanical impedance (EMI) and Lamb wave. In these methods, small PZT wafers are attached to the structure to be monitored. Those PZTs may work either as sensors or as transducers. In the direct piezoelectric effect, application of an electric field causes mechanical deformation resulting in an actuator. In the converse effect, application of a mechanical deformation causes an electric field resulting in a sensor. Both EMI- and Lamb wave–based methods use PZTs attached to the structure, which are excited within an appropriated frequency range to produce structural vibrations. The structural response signals are collected by acquisition systems and analyzed using different signal processing techniques (Hu and Yang, 2007; Lopes et al., 2000;

[1]Department of Electrical and Electronic, Federal Institute of Education, Science and Technology of Mato Grosso (IFMT), Campus de Cuiaba, Cuiaba, Brazil
[2]Department of Telecommunication Engineering, Universidade Estadual Paulista (UNESP), Campus de Sao Joao da Boa Vista, Sao Joao da Boa Vista, Brazil
[3]Department of Mechanical Engineering, Universidade Estadual Paulista (UNESP), Campus de Ilha Solteira, Ilha Solteira, Brazil
[4]Department of Aerospace Engineering, University of Michigan, Ann Arbor, MI, USA

Corresponding author:
Mario A de Oliveira, Department of Electrical and Electronic, Federal Institute of Education, Science and Technology of Mato Grosso (IFMT), Campus de Cuiaba, Cuiaba, MT 78005-200, Brazil.
Email: mario.oliveira@cba.ifmt.edu.br

Mal et al., 2005; Wang and Huang, 2001). These techniques demand knowledge of the pristine structure (called baseline). The baseline is the reference to identify possible structural damage when comparison with the unknown structural condition is carried out. More details about such techniques (EMI and Lamb wave) can be found in Giurgiutiu (2003, 2005, 2007), Giurgiutiu and Santoni-Bottai (2011), Giurgiutiu and Zagrai (2000), Lim et al. (2012), and Park et al. (2003, 2007).

Currently, computational tools along with digital/statistical signal processing techniques are essential for developing new SHM applications considering both time and frequency domain processing. Such techniques, along with new hardware and software, make SHM systems more autonomous and accurate for detecting structural faults (Cortez et al., 2012; Staszewski and Worden, 2004). In general, the signals obtained from the PZT carry important information of the structure's condition, but they arrive along with undesired spurious signals such as noise, displacement, and environmental interference. These signals, in most of the cases, have to be pre-processed before computing metrics. In that step, researchers are looking for normalization, tendency, outlier, noise, metrics, smoothing, and filtering process (De Oliveira et al., 2014; Silva et al., 2008; Staszewski, 2002; Staszewski et al., 2000). Some of these features will be removed and others will be incorporated during the implementation of damage detection system.

Papers in the literature have addressed the issue of using singularities for damage identification in the concept of the wavelet analysis. Some of those important approaches are summarized next. Robertson et al. (2003) proposed to identify a feature, extracted from a system's acceleration time histories, that indicates the presence of singularities and identifies when they occurred. This feature was based on the Holder exponent (Lipschitz exponent) what provides a measure of a signal's regularity. Therein, the wavelet transform was used to obtain a time-based Holder exponent function. Peng et al. (2003) proposed a method for fault diagnosis based on multifractal spectrum (singularity spectrum) based on the vibration signals obtained from rotating machinery. Multifractal spectrum was computed by the wavelet transform modulus-maxima (WTMM) and applied to analyze the experimental data of rub-impact, oil whirl, coupling misalignment, and imbalance faults. Peng et al. (2003) state that the multifractal spectrum can characterize the singularity property of the vibration signals well. In the same way, Staszewski and Robertson (2007) used the Lipschitz exponent analysis to investigate the acceleration response of a structure subject to a harmonic base excitation. Extraction of the Lipschitz exponent was performed using the Morlet wavelet transform for all of the in-axis data. According to the authors, the singularities were successful for identifying discontinuities. The discussion about identifying structural damage using singularities along with the wavelet transform can be further exploited in Staszewski and Robertson (2007). Nowadays, the effects of singularities, obtained from structural response signals, have been exploited along with singular spectrum analysis (SSA) as presented in Loh et al. (2010, 2011). Therein, the authors state that the singularities are related to either cracks or damage or by environmental changes. Hence, based on the aforementioned issues, this work addresses the damage identification based on analysis of residues from SSA decomposition. This analysis strategy appears to be very interesting considering the fact that noise components, extracted by SSA, may contain the effects of singularities. Considering that the signals obtained from the undamaged and damaged structural conditions have the same level of noise, the difference between both signals may be caused by damage (singularity), and it constitutes an excellent way to identify structural damage as presented here.

SSA has been used by some authors in the field of SHM especially in the last 4 years. Some important papers focusing on SSA for SHM approaches are reviewed next. Loh et al. (2010) used SSA to decompose the response signal obtained from reinforced concrete frames aiming to monitor permanent deformations in that structure. The damage was extracted exploring the high-frequency variability of SSA. Loh et al. (2011) developed a new method to continuously monitor the structural quality of the *Taiwan Arc*. This structure was subjected to different levels of nonlinear behavior caused by variations in environmental conditions. SSA and nonlinear principal component analysis (NPCA) were used to extract residual deformation. The work presented by Trendafilova (2012) addresses a new method exploring the inverse analysis and data modeling applied to nonlinear structural vibration. A statistical approach was conducted based on SSA to analyze the response signals obtained from a composite structure which was subjected to an initial stimulus and was left to vibrate on its own (free decay response–based method). The response signal was decomposed into principal components (PCs), which were used to discover a new oscillatory standard of structural response (Trendafilova, 2012). Muruganatham et al. (2013) used SSA to decompose a time series (vibration signals) obtained from slip in electrical motors. From the SSA, two sets of time series were obtained, periodic and nonperiodic (noise), and used to obtain prediction models aiming to prevent future faults. Garcia and Trendafilova (2014) used SSA applied to a vibration-based system which was applied to an experimental case study of a composite laminate beam. This method is based on the decomposition of the frequency domain structural variation response using new variables (PC). Different structural scenarios were clearly

distinguishable, and these were performed to identify delamination.

Based on the aforesaid, this article proposes a novel method for damage detection, applied to SHM, based on a new method of excitation/reception exploiting time series analysis through SSA. For this, an appropriated signal is used to excite the structure through a PZT, and another PZT is used as a sensor to receive the response signal as in the pitch–catch Lamb wave–based methods. However, the structure is excited using a large range of frequencies as used in the EMI-based method. An SSA algorithm is applied to the response signals, and the residues obtained between the original and reconstruct time series are used in ratios to improve the sensitivity of the root mean square deviation (RMSD) and correlation coefficient deviation metric (CCDM) which are sensitive indices used to detect damage. The proposed method was tested on an aluminum plate, and the results were analyzed considering different numbers of components used during the reconstruction procedure of the time series.

In short, the proposed method presents some similarities with the acoustic-ultrasonic technique proposed in Vary and Lark (1978), which explored a different method using a higher frequency range varying from 1.3 to 1.7 MHz. In the same way, Michaels and Michaels (2005) and Lu and Michaels (2005, 2009) proposed damage identification using diffused ultrasonic in a frequency range around 2 MHz. Biemans et al. (2001) proposed to excite the structure using a sine signal sweeping from 10 to 50 kHz with the ramp time of 0.01 s and amplitude of the excitation signal limited to 20 V. In comparison with those papers, the work presented here focuses on lower frequency signals (chirp) ranging from 0 to 250 kHz with amplitude limited to 5 V to excite a PZT, which is similar to EMI-based methods, and obtain structural response using another PZT, which is a characteristic of Lamb wave–based methods. In De Oliveira et al. (2013), the Savitzky–Golay filter was applied and damage indices were based only on CCDM. In Vieira Filho et al. (2011), the authors proposed a method based on the magnitude of the coherence function (MCF). Despite using similar idea for exciting the structure, the damage metric was based on computing the standard deviation from MCF, thereby using different metrics than the ones presented here.

In general terms, this article provides a new time domain approach to the SHM literature that is apparently more sensitive for damage detection than other similar methods, making an easier and precise choice of a practical damage threshold, essential for a more reliable damage identification, especially when assessing structures made up of composite materials. However, it does not consider temperature and load effects, which can be seen as a disadvantage. However, additional research is ongoing and preliminary results considering temperature and load effects are promising.

This article is organized as follows: first, a brief review of SSA is presented. Next, the time domain analysis technique based on the proposed method is shown and the test scenarios and experimental study are presented. This article concludes highlighting advantages and drawbacks of the proposed method.

SSA

Currently, SSA consists in one of the most important method applied to time series analysis. This method incorporates elements of classical time series analysis, digital signal processing, system dynamics, and multivariate statistics. The main idea behind the SSA consists in the decomposition of the original time series into a set of independent components from which three different characteristics can be extracted: trend, harmonic (oscillatory), and noise (Hassani, 2007; Mirmonemi et al., 2011). According to Golyandina et al. (2001), harmonic series are periodic or quasi-periodic series which can be either pure or amplitude-modulated. The noise component is any aperiodic series. The trend corresponds to a slowly varying additive component of the series in which the oscillations are removed or smoothed. SSA is a nonparametric method, meaning that the mathematical model of the dynamic system does not need to be computed. The spectral decomposition is based on the covariance matrix of Karhunen–Loeve (Mirmonemi et al., 2011). The SSA procedure can be developed in four steps (Hassani, 2007).

Step 1: time series decomposition

A multidimensional sequence $\{X(t)\}$ is extracted from the original one-dimensional time series (structural response signals) $\{Y(t): t = 1, \ldots, N\}$ as follows

$$X(t) = (Y(t), Y(t+1), \ldots, Y(t+L-1)) \quad (1)$$

where $t = 1, \ldots, K$, and K is the number of lagged vectors and is given by

$$K = N - L + 1 \quad (2)$$

where L is the window length, and it is defined as an integer such that $2 \leq L \leq N$. It is important to highlight that the design space can be understood by analyzing the spatial coordinates system based on the window presented in Figure 1. This figure also depicts the interrelationship among SSA, multi-channel SSA (M-SSA), and principal component analysis (PCA). The axes represent the spatial coordinate (PC label) *x, t*, and lag *s*, and the discrete values are labeled as *c, n*, and *j*, respectively (Ghil et al., 2002). For working with SSA, the design space is accomplished by setting C to 1, thereby making a special case of M-SSA, where C represents the number of channels for M-SSA. If $K = 1$, we have the traditional PCA technique. This subject is well

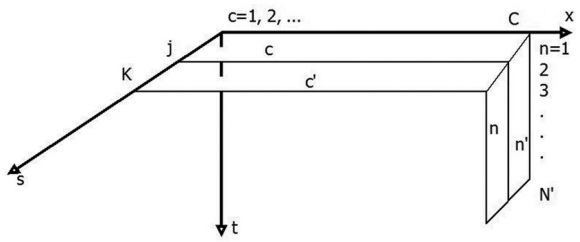

Figure 1. Window showing the design space for SSA, M-SSA, and PCA.

known in the literature, and further details can be found in Ghil et al. (2002).

Choosing the length of window (L) is one of the biggest challenges when working with SSA, mainly for complex series. On one hand, a large window, at least bigger than half of the series length, demands greater computational efforts. On the other hand, if a small window length is chosen, it is quite impossible to separate noise from the trend components. Sometimes, it is necessary to conduct several tests to find out which length is most useful. However, several researchers have applied statistical tests to obtain a systematic way for determining the best length of the window. One of them is the autocorrelation coefficient (Co), which for a signal Y(t) with N data points can be computed as follows

$$\mathrm{Co} = \frac{\sum_{t=1}^{N-1} (Y(t) - \bar{Y}(t))(Y(t+1) - \bar{Y}(t))}{\sum_{t=1}^{N} (Y(t) - \bar{Y}(t))^2} \quad (3)$$

where $\bar{Y}(t)$ represents the average of Y(t). Later on, we will present further details about the procedure of choosing of length L. The final result obtained from the first step is the trajectory matrix given by

$$\mathbf{X} = [X_1, X_2, \ldots, X_K] \quad (4)$$

The **X** resultant matrix is known as a Hankel matrix because all its elements along the diagonal i + j are constant and equal.

Step 2: singular value decomposition

The singular value decomposition (SVD) of the trajectory matrix (X) is

$$\mathbf{X} = \sum_{i=1}^{d} \sqrt{\lambda_i} U_i V_i^T \quad (5)$$

where $\{\lambda_i, i = 1, \ldots, d\}$ are the set of eigenvalues of the matrix $\mathbf{X}\mathbf{X}^T$; $\sqrt{\lambda_i}$ is the ith singular value of **X**; ($\sqrt{\lambda_i}$, U_i, V_i) are known as the ith eigentriple; $U_1, \ldots, U_d$ are called empirical orthogonal functions; and $V_1, \ldots, V_d$ are the PCs.

Step 3: grouping

This step consists of splitting the elementary matrices $\mathbf{X}_i$ into several groups. For this, let $I = \{i_1, \ldots, i_p\}$ be a group of indices $i_1, \ldots, i_p$. $\mathbf{X_I}$ corresponding to the group I is defined as $\mathbf{X_I} = \mathbf{X}_{i1} + \ldots + \mathbf{X}_{ip}$. Subsets can be obtained as follows

$$\mathbf{X} = \mathbf{X_{I1}} + \cdots + \mathbf{X_{Im}} \quad (6)$$

where **X** is the trajectory matrix. The procedure for choosing the sets $I_1, \ldots, I_m$ is called the eigentriple grouping.

Step 4: reconstruction

The diagonal averaging procedure transfers each group I into a time series, which is an additive component of the initial series Y(t). The result is the trajectory matrix corresponding to the series (Hassani et al., 2011). Applying the Hankelization procedure to all matrix components of equation (6) yields

$$\mathbf{X} = \tilde{\mathbf{X}}_{\mathbf{I1}} + \cdots + \tilde{\mathbf{X}}_{\mathbf{Im}} \quad (7)$$

where $\tilde{\mathbf{X}}_{\mathbf{I1}}$ corresponds to the Hankel matrix. This corresponds to the decomposition of the initial series Y(t) into a sum of m series

$$y(t) = \sum_{k=1}^{m} \tilde{y}_t^{(k)} \quad (8)$$

where $\tilde{Y}_T^{(k)} = \tilde{y}_1^{(k)} + \cdots + \tilde{y}_T^{(k)}$ corresponds to the matrix $\mathbf{X}_{Ik}$.

During the reconstruction procedure, each PC contributes part of the retained energy obtained from the original series. Obviously, if all components are added to the final series, it will practically contain the energy of the initial series. Another challenge for working with SSA consists of identifying how many components should be used in the reconstruction procedure. To try solving this, certain experimental tests should be conducted along with the analysis of eigenvalues to have good accuracy about how many components are necessary during the reconstruction process. This approach requires separation between noise components and others, and because our interest is focused on the residues, it is necessary to use a large number of components during the reconstruction process. Projection and visualization onto the reconstructed PCA subspace can be found in Garcia and Trendafilova (2014).

The residue of time series (r) can be computed considering the difference between both time series, the original and the reconstructed one, as follows

$$r(t) = Y(t) - \tilde{Y}_T^{(k)} \quad (9)$$

Certainly, a larger number of components in the reconstruction procedure assure smaller residues.

Proposed method

As aforementioned, the proposed approach presents features from both the EMI and Lamb wave methods, although there are also substantial differences. In relation to EMI, the differences consist in using an appropriate signal to set the excitation through the PZT transducer, while three other PZTs are used only as sensors for collecting the response signal from the structure. In this configuration, each sensor acquires the response signal separately similar to Lamb wave applications. However, the excitation signal, in terms of frequency and amplitude, varies as it does in the EMI method. The configuration used is also different from the Lamb wave approach which uses a pure tone excitation signal at high amplitude. The excitation signal used here is a chirp signal with low amplitude level (about 5 V). The basic concepts of the proposed methodology are based on the configuration shown in Figure 2.

Considering the issues aforesaid, the proposed methodology can be summarized as follows:

- *Step 1*: Four piezoelectric transducers are bonded to the structure to be monitored. In this configuration, transducer A operates as actuator for exciting the structure in an appropriate frequency range (chirp signal ranging from zero up to hundreds of hertz), and the other three transducers operate passively and separately as sensors (S1, S2, and S3). It is important to emphasize that at first, actuator A excites the structure and the S1 response is sampled and recorded. In a second step, the same excitation procedure is carried out and the S2 response is acquired. Finally, the same procedure is conducted and the S3 response is obtained. From this approach, the response signals are obtained separately for each PZT sensor, thereby allowing the proposed method to work on each response signal separately.
- *Step 2*: The structural response signals are decomposed, in the time domain, using the algorithm of the SSA. This procedure is carried out using MATLAB® software. As aforementioned, SSA procedure corresponds to four steps: time series decomposition, SVD, grouping, and reconstruction. It is important to point out that SSA provides good distinction among three different groups such as trend, oscillatory (harmonic), and noise. Those features are extremely important for the present work because we are focusing on the analysis of the noise components. Structural damage may cause a singularity in the response signal. This singularity is presented in the noise component rendering it one important quantity to be analyzed. Thus, during the process of reconstruction of the time series, this approach will use only the features of the harmonic and trend components.
- *Step 3*: The residues are obtained from the difference between the reconstructed series and the original one.
- *Step 4*: The residues are then used to identify the structural damage through the statistical indices such as RMSD and CCDM. The RMSD index is computed using equation (10), considering the residues for the healthy condition as the reference (baseline)

$$\mathrm{RMSD} = \sum_{n}^{N} \sqrt{\frac{(r_{n,u} - r_{n,h})^2}{(r_{n,h})^2}} \tag{10}$$

where $r_{n,u}$ and $r_{n,h}$ are the residues considering unknown and healthy (baseline) conditions, respectively. The CCDM is computed according to

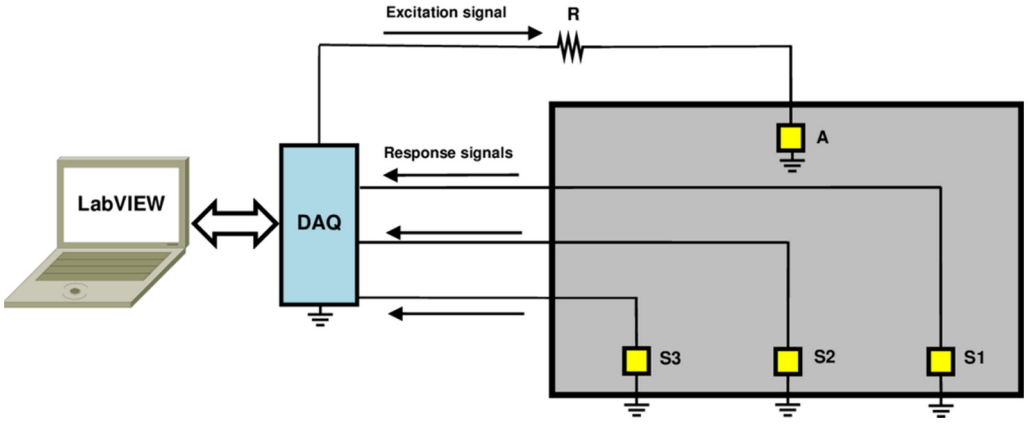

Figure 2. Proposed diagram for damage identification.

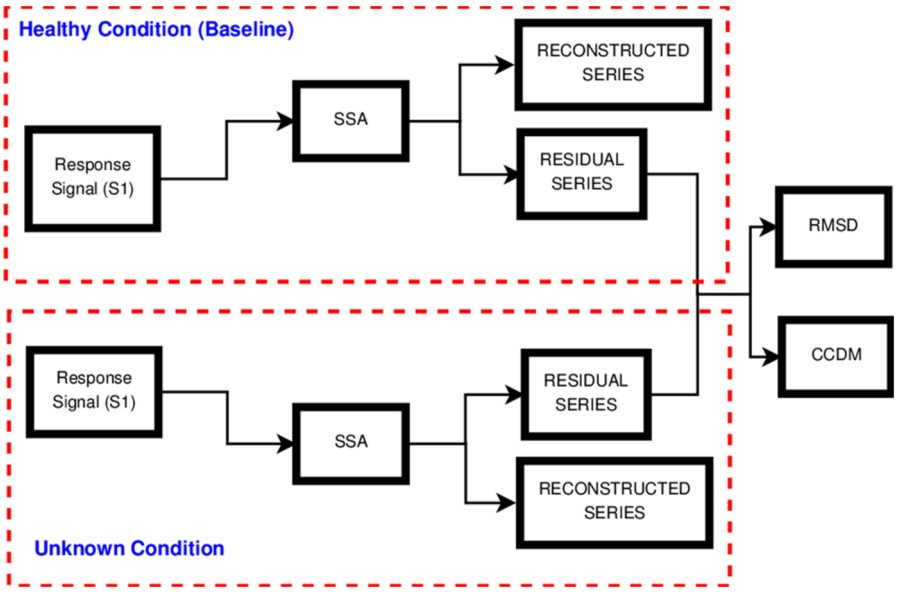

Figure 3. Diagram of the proposed method based on SSA.

$$\mathrm{CCDM} = 1 - \left| \frac{\sum_{n}^{N} (r_{n,h} - \bar{r}_h)(r_{n,h} - \bar{r}_u)}{\sqrt{\sum_{n}^{N} (r_{n,h} - \bar{r}_h)^2} \sqrt{\sum_{n}^{N} (r_{n,u} - \bar{r}_u)^2}} \right| \quad (11)$$

where $\bar{r}_h$ and $\bar{r}_u$ are the averages of residues for the healthy (baseline) and the unknown structural conditions, respectively.

In summary, the entire procedure for sensor 1 (S1) is presented in Figure 3. Similar procedures are also conducted for the two other sensors (S2 and S3).

Experimental setup

The acquisition system used in this work is controlled from the software developed by Baptista and Vieira Filho (2009) on the LabVIEW® platform and also manages the multifunctional data acquisition (DAQ) device model USB-6259. The excitation signal x is used to excite the actuator and consequently the structure (Figure 2). The DAQ provides the signal x[n] and y[n] in discrete form.

Experimental tests were carried out using the system shown in Figure 2. Four piezoceramic wafers PSI-5H4E of 20 mm × 20 mm × 0.267 mm were bonded to an aluminum plate of 500 mm × 230 mm × 0.267 mm in different positions as shown in Figure 4. PZT (A) is used as actuator and S1, S2, and S3 are used as sensors. Four damage states (D1, D2, D3, and D4) were simulated by bonding a 4 mm × 2 mm steel nut of about 10 g to the structure at different positions (Figure 4).

At first, the set PZT was excited using a chirp signal ranging from 0 to 250 kHz and 5 V of amplitude. The

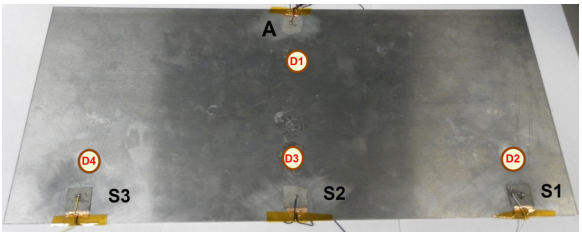

Figure 4. Experimental setup containing PZTs and damage.

structural response signals were sampled at a rate of 1.25 Msample/s. Hence, each sampled signal is composed of 65,536 samples corresponding to 52.4 ms duration. The response signals were obtained from the structure in the healthy condition (baseline) for all three sensors. Second, four damage states, using a steel nut of 4 mm × 2 mm and about 10 g, were simulated (D1, D2, D3, and D4) on the structure, and for each damage, the response signals were obtained from all of the sensors. After removing the damage, new response signals were obtained considering the structure in healthy condition again (repaired).

Results and discussions

Figure 5 depicts three time-response signals, obtained from sensor S1 considering the following conditions: damage D1, damage D2, and the healthy condition. The percentage change in the signal, computed between signals for damage D1 and the healthy signal, is subtle reaching roughly 4.27% when computed via the root mean squared error (RSME). In the same way, the RSME metric computed between signals for healthy and damage D2 reached 3.84%.

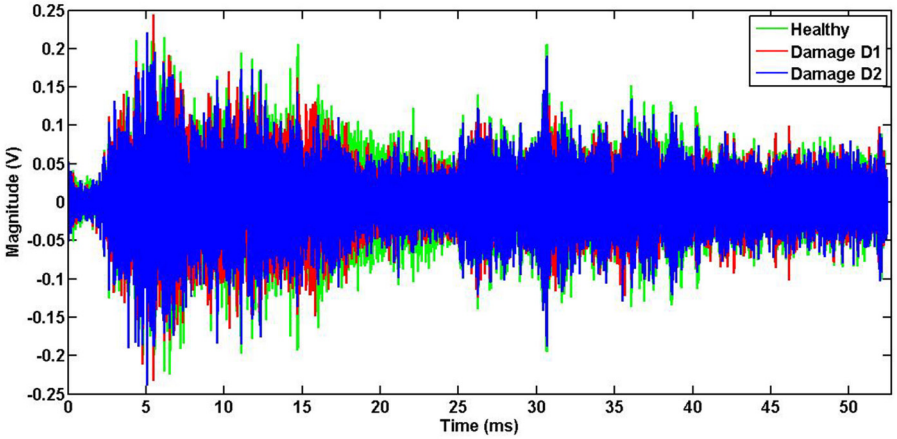

Figure 5. Response signals obtained from sensor S1 considering three different structural conditions: damage D1, damage D2, and healthy condition.

The SSA procedure was performed for each measured signal. The first step consists of decomposing the time series into trajectory matrices. During this step, it is necessary to choose the length of the window for decomposing the series. In this approach, the autocorrelation test (equation (3)) was computed to provide good evidence for the best choice for length L. Analytically, the length of window (L) is computed such that the points of different lagged vectors can be considered to be linearly independent. The idea is that window length L is chosen to be equal to the correlation length when the sample autocorrelation function given by equation (3) crosses the confidence interval of 95% (red lines in Figure 6) for the first time. After this procedure, the lagged vectors of length L can be considered to be independent, which enables each vector to be analyzed separately. From a practical point of view, researchers are looking for points around the zero crossing, and the first time crossing zero has been adopted in several works (Loh et al., 2011). The best choice may be around the zero crossing and not exactly at the crossing point. In our particular case, we also adopted the zero crossing because it makes the window choice much easier. Experimentally, the structural response signal obtained from sensor S1, for instance, was used to compute the autocorrelation function by equation (3). However, any crossing by zero or a neighborhood of zero may be considered possible points of analysis within the autocorrelation test since any choice is within the adopted confidence interval. Figure 6(a) shows the first zero crossing nearest to 4 lag which can be considered an excellent point to choose the length of the window. However, one small window length cannot provide good separation among the tendency, harmonic, and noise components. After several lengths of window tested, the 600 lag, as shown in Figure 6(b), was adopted. This resulted in statistical indices (RMSD and CCDM) that are more uniform when the damage variations were being performed. Overall, small variations in the window length would cause only an insignificant change in the results (RMSD and CCDM metrics) for the proposed approach.

In the second step, the SVD was conducted considering the length of the window to be 600. The percentage of eigenvalue as a function of the first 30 eigenvalues is presented in Figure 7. It is notable that during the reconstruction procedure, each PC contributes with part of the retained energy obtained from the original series. In general, the number of representative components can be determined by analyzing the percentage of the explained variance by each eigenvalue. Obviously, if all components are added to the final series, it will contain all the energy of the initial series. As a consequence, a greater number of eigenvalues are required to obtain the reconstructed signal as close as possible to the original signal. According to Hassani (2007), pairs with almost equal leading singular values (plateau) correspond to harmonic components of the series: eigentriple pairs 1–2, 3–4, 5–6, for instance, are related to harmonics with specific periods.

Figure 8 depicts the relationship among the latest eigenvalues (last five ones) computed from the response signal for S1 considering the healthy structural condition. As aforementioned, pairs with almost equal leading singular values (plateau) correspond to harmonic components of the series (eigentriple pairs 596–597 and 599–600 in Figure 8, for instance) with specific periods. On the contrary, the 598 eigenvalue is not related to any another pair. Ungrouped eigenvalues which do not reveal any plateaus are good candidates for noise components. This result is very interesting because noise components tend to be more susceptive to aggregate damage features from the structural signal response which may contain the effects of singularities as highlighted throughout this article.

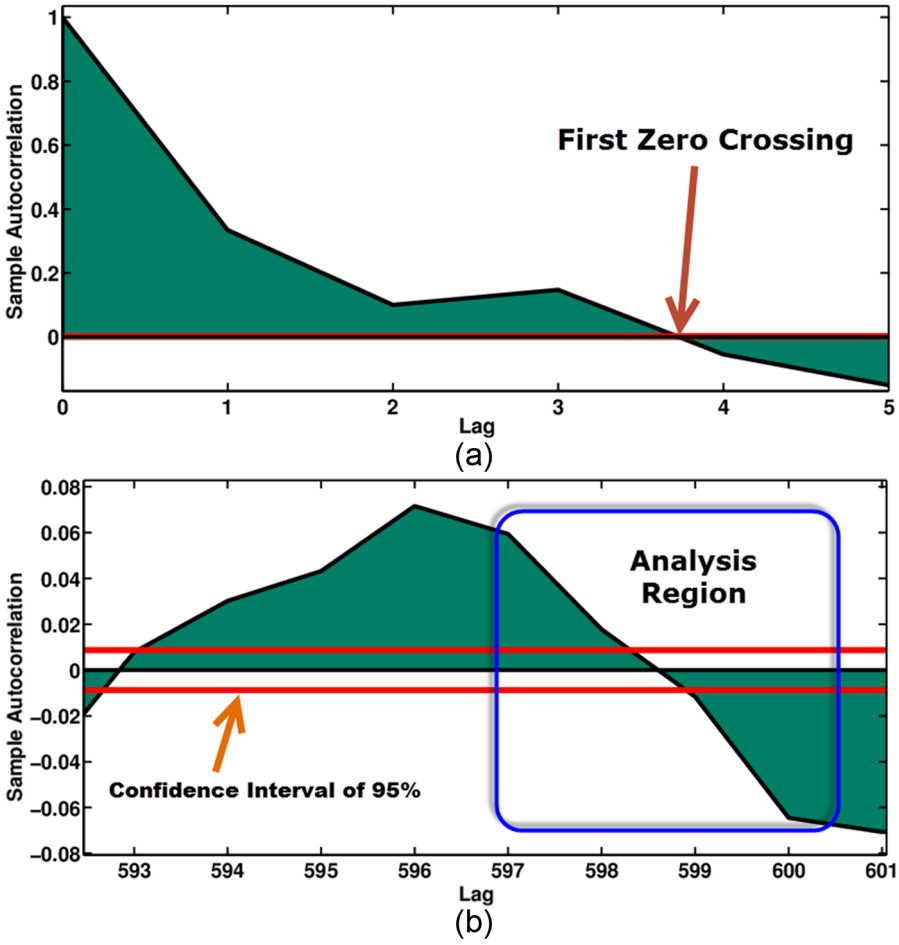

Figure 6. Autocorrelation in the function of lag: (a) first zero crossing and (b) adopted analysis region.

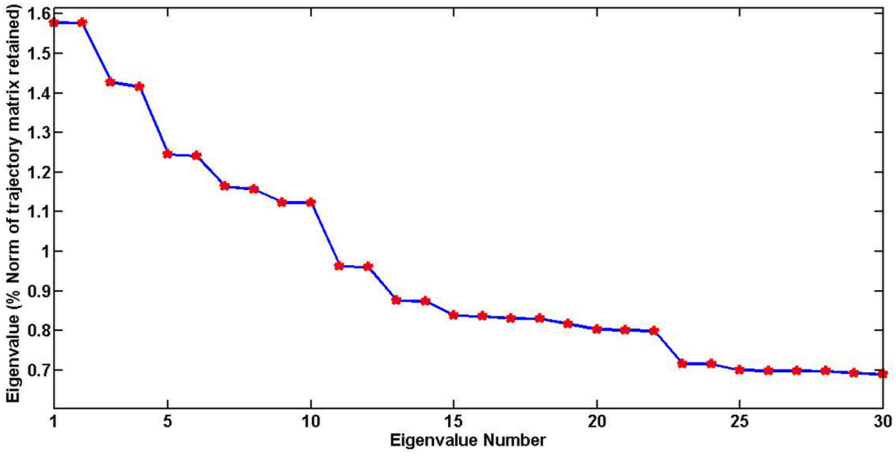

Figure 7. Norm of the trajectory matrix as a function of the eigenvalues.

Figure 9 shows more details about the relation of the singular values of the two eigentriples of a harmonic series which are often very close to each other. An analysis of the pairwise scatterplots of the singular vectors allows one to visually identify those eigentriples that correspond to the harmonic components of the series, provided these components are separable from the noise component. Harmonic components tend to form regular polygons because these components are composed of sine/cosine sequences. The scatterplots of

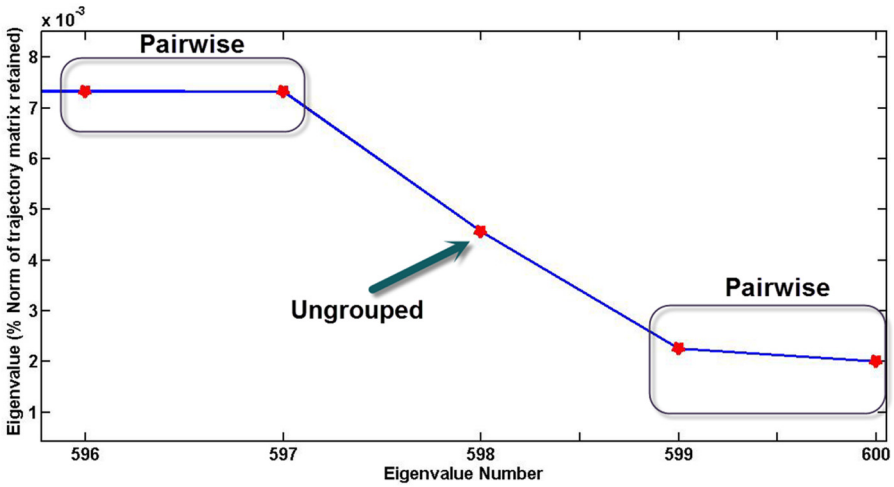

Figure 8. Norm of the trajectory matrix as a function of the eigenvalues highlighting the ungrouped 598 eigenvalue.

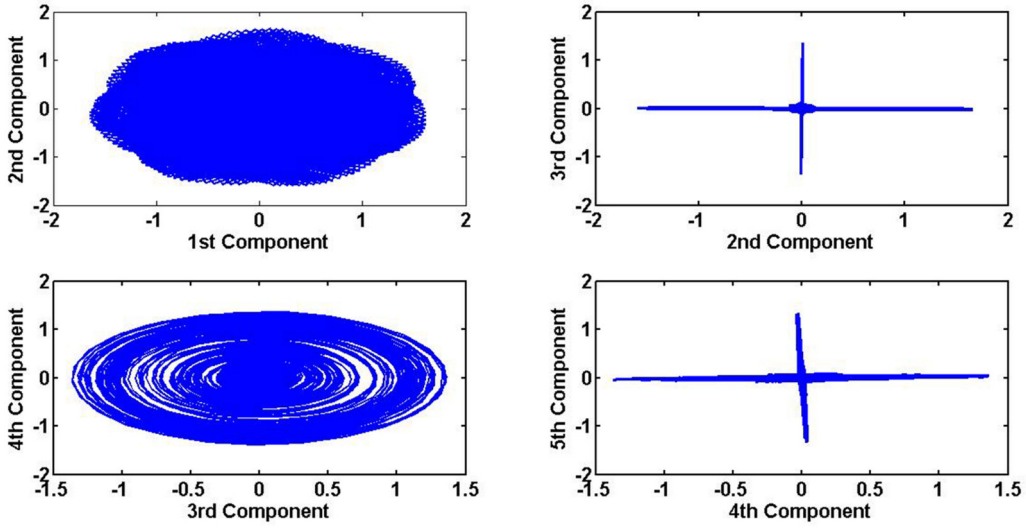

Figure 9. Scatterplot considering different compositions of the first eigentriples.

second with first and third with fourth components show strong evidence about the harmonic component as was expected based on the results presented in Figure 9. However, the scatters considering third with second and fourth with fifth components show that they do not have relations between their singular values as was expected because they have been related already to other singular values. In general, the harmonic and tendency components retain almost all of the energy of the eigenvalues as compared with the noise component.

Similar analyses were conducted considering the last components (Figure 10). These components tend to contain noise features that are the target of this work. Scatterplots considering the 596th with 597th and 598th with 599th components show small relations of singular values, whereas the 597th with 598th and 598th and 599th relations were decreased. An important fact is that the 598th component does not present a relation with neither the 597th nor the 599th. This means that this component has greater probability of being a noise component.

Figure 11 shows the decomposed series for the first four components. All of them have the same standard, except the displacement in the x-axis, and these features constitute once more the idea of the harmonic components. Figure 12 shows different results from those that were presented in Figure 11. The 597th component has a few features as those presented in Figure 11, whereas in the three those standards vanished, and these signals behave more like noise.

Based on these results, the reconstruction of time series was conducted considering a different number of components. At first, the first 599 components (the last one was left out) were considered; later on,

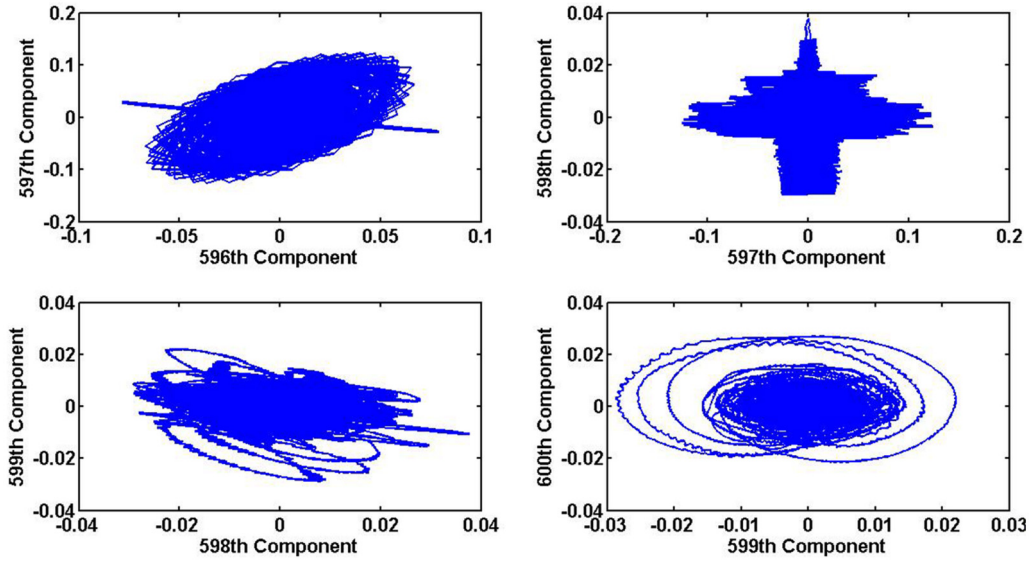

Figure 10. Scatterplot considering different compositions of the last eigentriples.

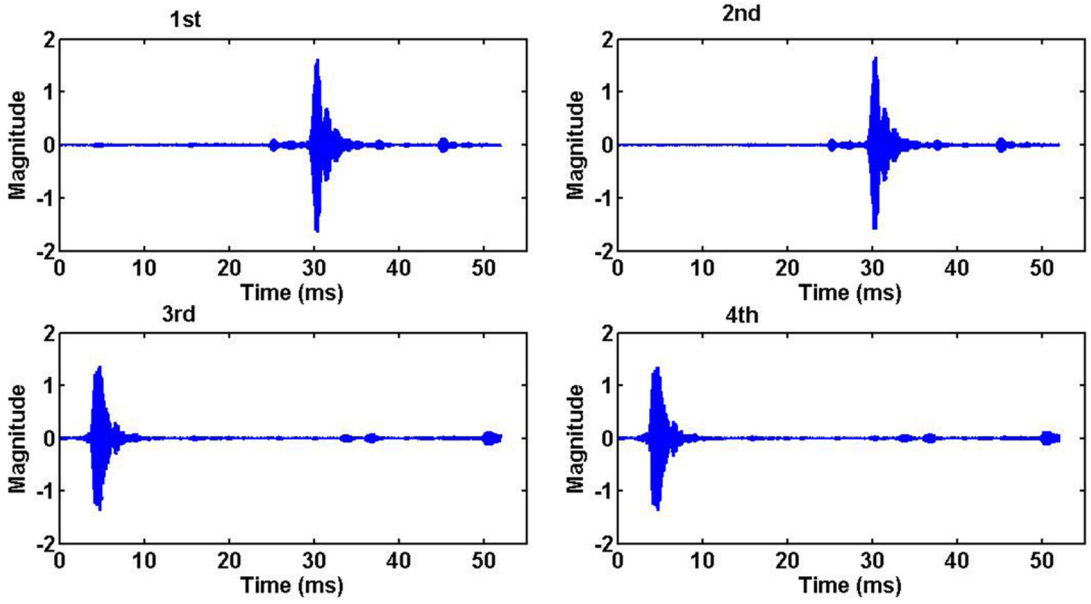

Figure 11. Principal components related to the first four eigentriples.

the results considering the effects of component numbers will be presented for the damage detection procedure as well. The residues were also computed using equation (9). Figure 13(a) shows the original and reconstructed time series for S1 under the healthy condition, whereas Figure 13(b) presents the resultant residues from the reconstruction procedure. It is almost impossible to observe the difference between both series (Figure 13(a)), and as a consequence, the residue has a low amplitude. Residues also were calculated from the time series obtained under healthy, damaged (D1, D2, D3, and D4), and repaired structural conditions for each sensor (S1, S2, and S3), and these were used to compute the statistical metrics RMSD and CCDM.

Using the first 599 components during the reconstruction process (only the last one was left out), the residues were computed and subsequently the statistical indices. Figure 14(a) and (b) shows both RMSD and CCDM for each sensor (S1, S2, and S3) considering all structural conditions. This figure shows only one case of the repaired condition since the other healthy condition cases were similar. All indices were normalized considering the repaired condition as a reference.

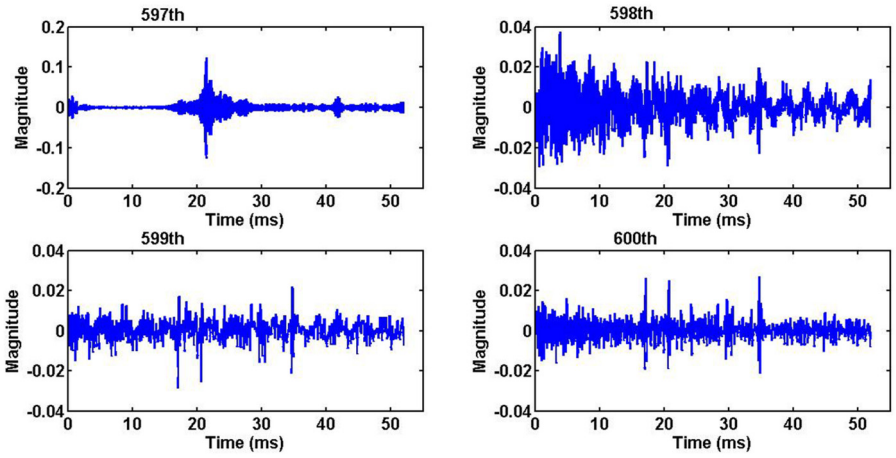

Figure 12. Principal components related to the last four eigentriples.

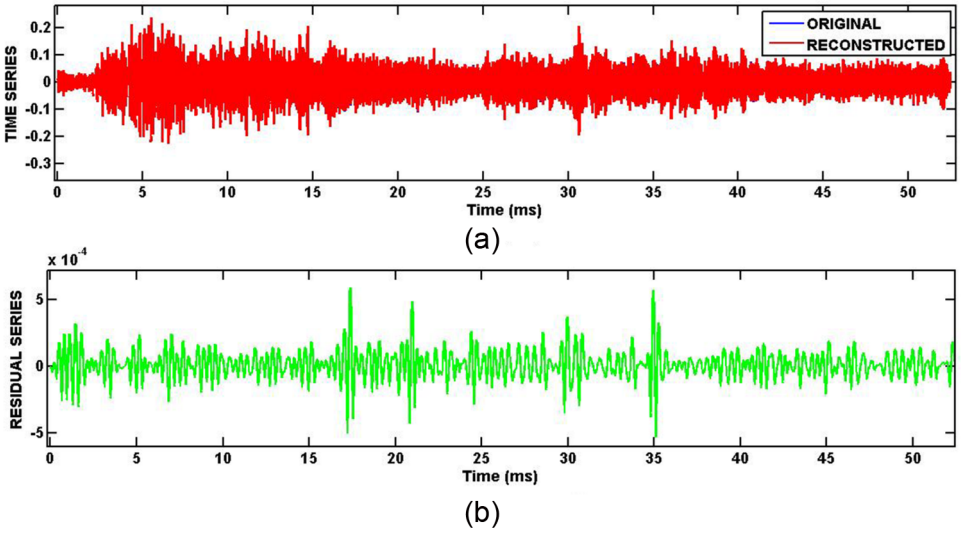

Figure 13. (a) Original and reconstructed time series obtained from structural response and (b) residue.

From Figure 14, it can be realized that there are significant differences among the repaired and damaged conditions in both RMSD and CCDM indices. The RMSD indices for damaged structural conditions are higher than those for the repaired structure, at least 10 times, whereas for the CCDM those differences were much higher, more than 250 times, resulting in excellent features for damage detection. The structural damage can be easily detected by all sensors using different thresholds. As expected, damage D1 was detected by all sensors with high sensitivity. Sensor S1 is more sensitive for damage D2 than damage D3 and damage D4. Sensor S2 also detected damage D3, and it has good features in terms of localization considering the CCDM indices, whereas sensor S3 presented good results, in terms of localization, for the RMSD. Moreover, sensor S2 has good sensitivity mainly for the CCDM indices when compared to others. Likely this is because sensor S2 is placed in the same line of actuator A.

Analyzing the overall results, we can point out that all the sensors were very responsive to damage D1. Because damage D1 is placed close to sensor A (actuator), where the forced vibration is the strongest, the response signal is greatly attenuated by D1 before reaching sensors S1, S2, and S3. For example, the percentage change in the signal for S1, computed between signals for damage D1 and the healthy baseline signal, is roughly 4.27% when computed via the RSME. However, when excitations signals reach damages D2, D3, and D4, those signals are already of low amplitude (due to being far away from the actuator), and such damage does not cause huge attenuations in those signals before they reach sensors S1, S2, and S3. To prove the point, the RSME metric computed for S1, considering signals for healthy and damaged D3, hit only 3.84%. In short, the nearer the actuator is to the damage, the greater the attenuation caused in the structural response signal caused by the damage and, as a

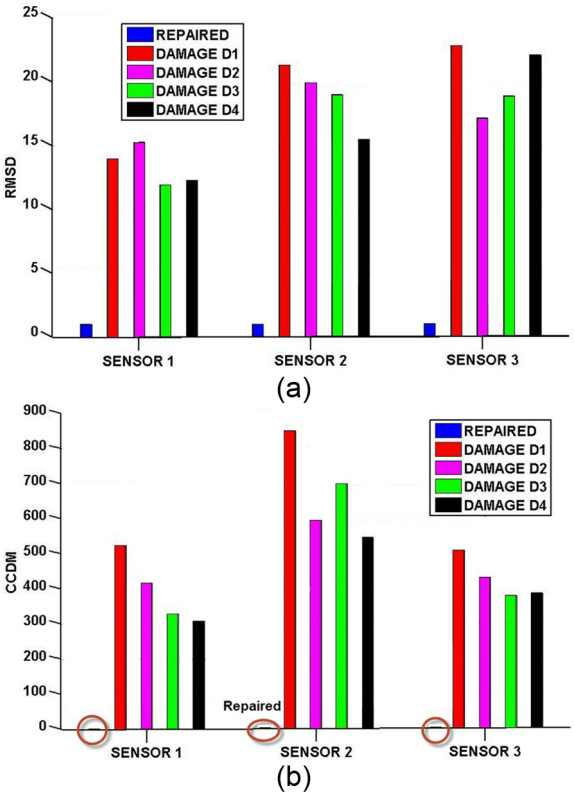

Figure 14. Statistical metrics including various structural conditions for all sensors: (a) RMSD and (b) CCDM.

consequence, the greater the difference between the healthy and damaged structural responses, therefore raising the percentage change in the signal.

As mentioned before, there are two big challenges when working with the SSA method: the length of window and the number of components used in the reconstruction procedure. For solving the first one, this approach adopted the autocorrelation method to decide which length would be better considering the zero crossing. For the second one, the choice was conducted after intensive experimental tests. Figure 15(a) to (c) shows the results for RMSD indices obtained during the reconstruction of the time series considering the first 599, 598, 597, 596, and 595 components. This means that only 0.1%, 0.2%, 0.3%, 0.4%, and 0.5% of the components are considered as the residues (left out), respectively. The structural conditions adopted are the same as presented before, and the results were normalized using the repaired condition as a reference. Figure 15 shows the sensitivity of the RMSD indices. The features kept the same standards, and any or all of the RMSD (residues) could be used during the damage detection procedure, keeping the same levels of confidence.

A similar procedure was also conducted for CCDM indices considering 0.1%, 0.2%, 0.3%, 0.4%, and 0.5% of the components as the residues. Those results are presented in Figure 16. The results presented in Figure 16 are totally similar for any CCDM indices, performing excellent sensitivity for damage detection and keeping a high level of confidence and accuracy. Thus, both RMSD and CCDM indices can be computed from the residues of SSA method to detect structural damage performing an excellent sensitivity and confidence when applied to SHM systems based on time domain analysis. The small variation in the number of components used during the reconstruction process of time series is meaningless for damage detection within the context of this approach as was previously shown. It is important to mention that comparing the results obtained here with that of previous researches in the literature is quite difficult because we do not have many approaches focused on using a similar scenario, which can lead to an unfair comparison.

Conclusion

This work presented a novel method for damage identification for structures by exploiting a technique based on the residues obtained from SSA. The procedure of actuation and sensing of signals from a set of PZTs mounted on a structure constitutes a novel approach in the sense that the approach incorporates features from both the EMI and Lamb wave methods. This new method along with the time series approach using the residues from SSA constitutes a unique feature, a highlight of this approach. In order to verify the effectiveness of the proposed method, experimental tests were conducted in an aluminum plate. An important note that can be highlighted from these tests is the high sensitivity of RMSD (at least 10 times) and CCDM (more than 250 times) when comparing the damaged structure conditions to the healthy condition, thereby providing a high level of confidence and accuracy for structural damage detection. Moreover, the proposed method may be able to present good results in terms of the position of the damage on structures considering both RMSD and CCDM indices working together.

Another interesting point to be mentioned is the choice of the number of components during the time series reconstruction process. As shown, the results are quite stable mainly for the CCDM index and less for RMSD index. This gives us good results even considering different numbers of components adopted during the reconstruction process. Although there is a significant number of eigenvalues/PCA being computed, the computational cost does not constitute a drawback because most SHM computations are carried out offline. Furthermore, computing eigenvalues/PCA has become only a very minor task for modern computers. To prove the point, the total demanded time in this application was only 56.34 s using a laptop running a developed application in MATLAB 7.10.0®/Windows 7®. The hardware setup was Intel dual-core i5-2410M CPU at 230 GHz and 18 GB of memory.

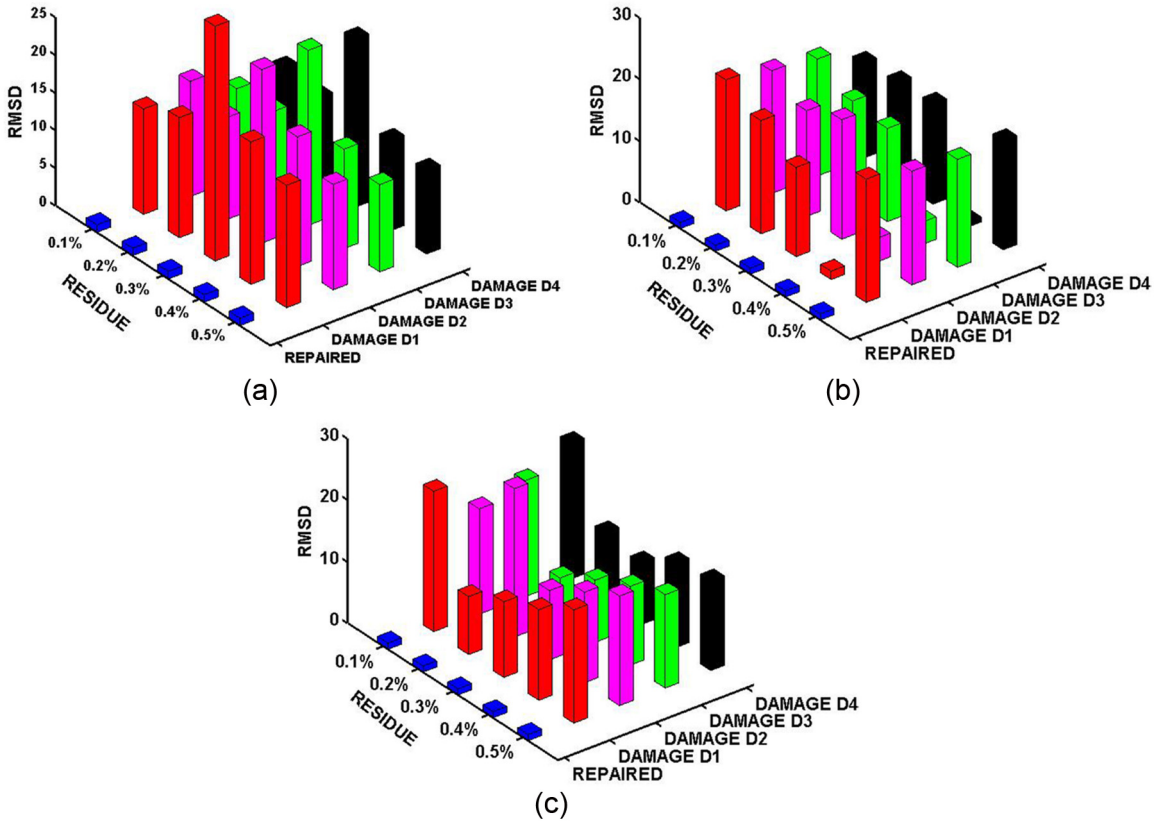

Figure 15. RMSD indices considering different numbers of principal components, which are considered as the residues, and various structural conditions: (a) sensor S1, (b) sensor S2, and (c) sensor S3.

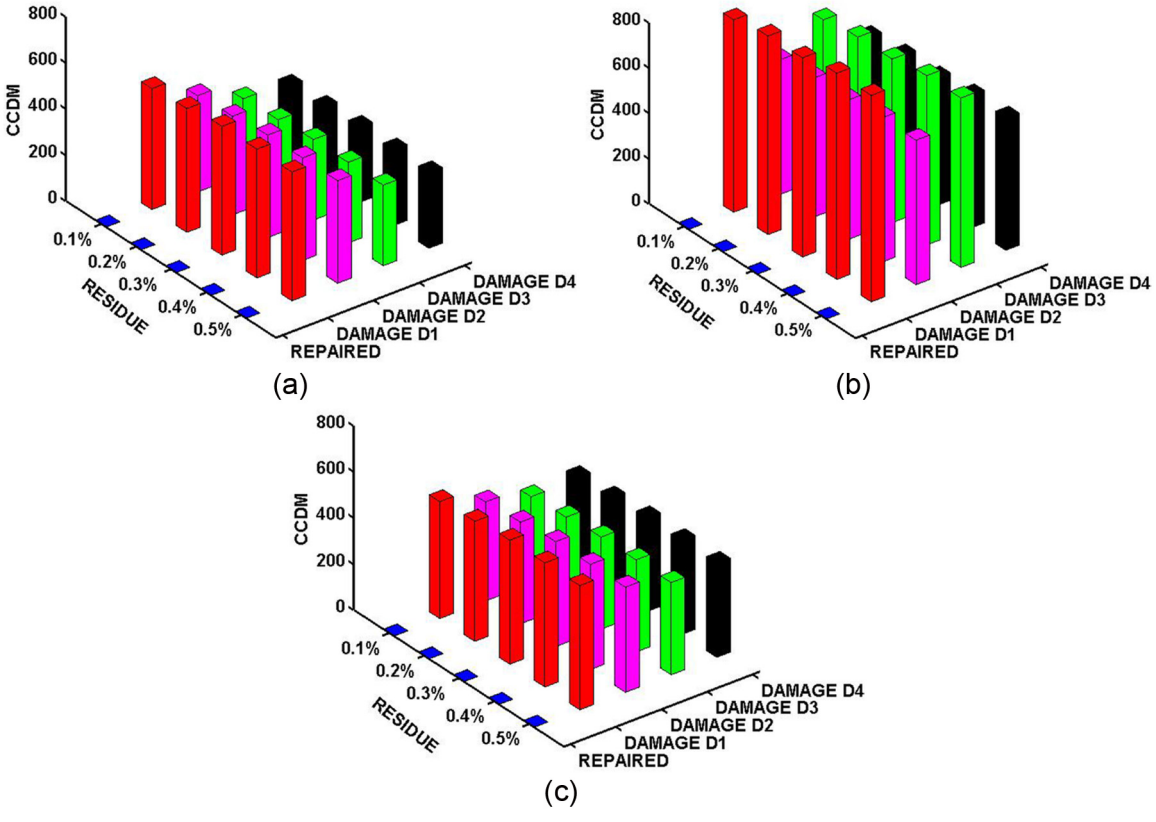

Figure 16. CCDM indices considering different numbers of principal components, which are considered as the residues, and various structural conditions: (a) sensor S1, (b) sensor S2, and (c) sensor S3.

Also, this high sensitivity may make the proposed method convenient in applications for which other methods present low sensitivity. However, it is important to remark that techniques which use PZT transducers applied to SHM are highly influenced by environmental conditions during the structural damage detection procedure, becoming one of the biggest challenges for SHM system developers. In this context, environmental changes have strong effects in this analysis which may cause serious errors (false alarms) during the process of identifying structural damage. Hence, this approach needs temperature compensation when working with temperatures different from the ambient (around 25°C).

The results demonstrate that the approach using the residues from SSA can be useful for this kind and size of damage and can be used to categorize damage and location. To date, we can only guarantee the capabilities of the method for damage identification and size/type estimation in terms of rather large size as defined here. Smaller damage sizes will form future investigations. However, the simulated damage represents only negligible increment of structural mass when compared to the total mass of the structure, which is compatible with real damage. Regardless, we believe that the example presented here demonstrates the effectiveness of the proposed method making it an excellent approach for SHM applications.

Acknowledgements

The authors are grateful to the reviewer's valuable comments that improved the manuscript.

Declaration of Conflicting Interests

The author(s) declared no potential conflicts of interest with respect to the research, authorship, and/or publication of this article.

Funding

The author(s) disclosed receipt of the following financial support for the research, authorship, and/or publication of this article: This work was supported by the CNPq, Brazilian Research Agency (Grants 248665/2013-8 and 306207/2013-3), and the University of Michigan through the Kelly Johnson Collegiate Chair Fund.

References

Baptista FG and Vieira Filho J (2009) A new impedance measurement system for PZT-based structural health monitoring. *IEEE Transactions on Instrumentation and Measurement* 58(10): 3602–3608.

Biemans C, Staszewski WJ, Boller C, et al. (2001) Crack detection in metallic structures using broadband excitation of acousto-ultrasonics. *Journal of Intelligent Material Systems and Structures* 12: 589–597.

Cortez NE, Vieira Filho J and Baptista FG (2012) A new microcontrolled structural health monitoring system based on the electromechanical impedance principle. *Structural Health Monitoring* 12(1): 14–22.

De Oliveira MA, Vieira Filho J, Lopes V Jr, et al. (2013) A novel time-domain technique for damage detection applied to SHM using Savitzky-Golay filter. In: *Proceeding of the 9th international workshop on structural health monitoring (IWSHM)*, Stanford, CA, 10–12 September, vol. 1, pp. 996–1003. Lancaster, Pennsylvania, DEStech Publication, Inc.

De Oliveira MA, Vieira Filho J, Lopes V Jr, et al. (2014) Damage detection based on electromechanical impedance principle and principal components. In: *Proceeding of the IMAC: a conference and exposition on structural dynamics*, Garden Grove, CA, 11–14 February 2013, vol. 7, pp. 307–315. New York: Springer.

Garcia D and Trendafilova I (2014) A multivariate data analysis approach towards vibration analysis and vibration-based damage assessment: application for delamination detection in a composite beam. *Journal of Sound and Vibration* 333(25): 7036–7050.

Ghil M, Allen MR, Dettinger MD, et al. (2002) Advanced spectral methods for climatic time series. *Reviews of Geophysics* 40(1): 1–40.

Giurgiutiu V (2003) Lamb wave generation with piezoelectric wafer active sensors for structural health monitoring. In: *Proceedings of the SPIE 5056, smart structures and materials*, San Diego, CA, 11 March, vol. 5056.

Giurgiutiu V (2005) Tuned Lamb wave excitation and detection with piezoelectric wafer active sensors for structural health monitoring. *Journal of Intelligent Material Systems and Structures* 16(291): 291–305.

Giurgiutiu V (2007) *Structural Health Monitoring: With Piezoelectric Wafer Active Sensors*. 1st ed. New York: Academic Press, 760 pp.

Giurgiutiu V and Santoni-Bottai G (2011) Structural health monitoring of composite structures with piezoelectric-wafer active sensors. *AIAA Journal* 49(3): 565–581.

Giurgiutiu V and Zagrai A (2000) Characterization of piezoelectric wafer active sensors. *Journal of Intelligent Material Systems and Structures* 11(12): 959–976.

Golyandina N, Nekrutkin V and Zhigljavsky (2001) *A Analysis of Times Series structures SSA and Related Techniques*. 1st ed. London: Charpman &Hall/CRC, 320 pp.

Hassani H (2007) Singular spectrum analysis: methodology and comparison. *Journal of Data Science* 5(2): 239–257.

Hassani H, Xu Z and Zhigljavsky A (2011) Singular spectrum analysis based on the perturbation theory. *Nonlinear Analysis: Real World Applications* 12(5): 2752–2766.

Hu Y and Yang Y (2007) Wave propagation modeling of the PZT sensing region for structural health monitoring. *Smart Materials and Structures* 16(3): 706–716.

Lim SI, Liu Y and Soh CK (2012) Comparative study of electromechanical impedance and Lamb wave techniques for fatigue crack detection and monitoring in metallic structures. In: *Proceeding of the SPIE 8345, sensors and smart structures technologies for civil, mechanical, and aerospace systems*, San Diego, CA, 11 March, vol. 8345.

Loh CH, Chen CH and Hsu TY (2011) Application of advanced statistical methods for extracting long-term

trends in static monitoring data from an arch dam. *Structural Health Monitoring* 10(6): 587–601.

Loh CH, Chen CH and Mao CH (2010) Detecting seismic response signals using singular spectrum analysis. In: *Proceeding of the SPIE 7647, sensors and smart structures technologies for civil, mechanical, and aerospace systems*, San Diego, CA, vol. 7647, pp. 1–12. Available at: http://proceedings.spiedigitallibrary.org/proceeding.aspx?articleid=757880

Lopes V Jr, Park G, Cudney HH, et al. (2000) Impedance-based structural healthy with artificial neural networks. *Journal of Intelligent Material Systems and Structures* 11(3): 206–214.

Lu Y and Michaels JE (2005) A methodology for structural health monitoring with diffuse ultrasonic waves in the presence of temperature variations. *Ultrasonics* 43: 717–731.

Lu Y and Michaels JE (2009) Feature extraction and sensor fusion for ultrasonic structural health monitoring under changing environmental conditions. *IEEE Sensors* 9(11): 1462–1471.

Mal A, Ricci F, Banerjee S, et al. (2005) A conceptual structural health monitoring system based on vibration and wave propagation. *Structural Health Monitoring* 4(3): 283–293.

Michaels JE and Michaels TE (2005) Detection of structural damage from the local temporal coherence of diffuse ultrasonic signals. *IEEE Transactions on Ultrasonics, Ferroelectrics, and Frequency Control* 52(10): 1769–1782.

Mirmonemi M, Lucas C, Araabi BN, et al. (2011) Recursive spectral analysis of natural time series based on eigenvector matrix perturbation for online applications. *IET Signal Processing* 5(6): 15–526.

Muruganatham B, Sanjith MA, Krishnakumar B, et al. (2013) Roller element bearing fault diagnosis using singular spectrum analysis. *Mechanical Systems and Signal Processing* 35(1–2): 150–166.

Park G, Lee JJ, Yun CB, et al. (2007) Electro-mechanical impedance-based wireless structural health monitoring using PCA-data compression and k-means clustering algorithms. *Journal of Intelligent Material Systems and Structures* 19(4): 509–520.

Park G, Sohn H, Farrar C, et al. (2003) Overview of piezoelectric impedance-based health monitoring and path forward. *Shock and Vibration Digest* 35(6): 451–463.

Peng Z, He Y, Guo D and Chu F L (2003) Wavelet Multifractal Approaches for Singularity Analysis of Vibration Signals, *Key Engineering Materials*, Vols. 245–246, pp. 565–570.

Robertson AN, Farrar CR and Sohn H (2003) Singularity detection for structural health monitoring using Hölder exponents. *Mechanical Systems and Signal Processing* 17: 1163–1184.

Silva S, Dias Junior M and Lopes V Jr (2008) Structural health monitoring in smart structures through time series analysis. *Structural Health Monitoring* 7(3): 231–244.

Staszewski JW (2002) Intelligent signal processing for damage detection in composite materials. *Composites Science and Technology* 62(7–8): 941–950.

Staszewski JW and Robertson AN (2007) Time–frequency and time–scale analyses for structural health monitoring. *Philosophical Transactions of the Royal Society A* 356: 449–477.

Staszewski WJ and Worden K (2004) *Health Monitoring of Aerospace Structures: Smart Sensor Technologies and Signal Processing: An Introduction to Damage Prognosis*. 1st ed. Munich: John Wiley & Sons, 266 pp.

Staszewski WJ, Read IJ and Foote PD (2000) Damage detection in composite materials using optical fibers: Recent advances in signal processing. In: *Proceeding of the SPIE 3985, smart structures and materials 2000: Smart structures and integrated systems*, Newport Beach, CA, vol. 3985, pp. 261–270. Available at: http://proceedings.spiedigitallibrary.org/proceeding.aspx?articleid=924187

Trendafilova I (2012) An inverse vibration-based approach towards modelling and damage identification in nonlinearly vibrating structures. Application for delamination detection in a composite beam. *Journal of Physics: Conference Series* 382(1): 12–30.

Vary A and Lark RF (1978) Correlation of fiber composite tensile strength with the ultrasonic stress wave factor. In: *Proceeding of Spring conference sponsored by the American Society for Nondestructive Testing*, New Orleans, LA, 3–7 April, pp. 1–21.

Vieira Filho J, Baptista FG and Inman DJ (2011) A PZT-based technique for SHM using the coherence function. In: *Proceedings of the 29th IMAC: a conference on structural dynamics*, Jacksonville, FL, vol. 1, pp. 111–118. New York: Springer 07 February 2011.

Wang XD and Huang GL (2001) Wave propagation in electromechanical structures: induced by surface-bonded piezoelectric actuators. *Journal of Intelligent Material Systems and Structures* 12(2): 105–115.